Published in final edited form as:
Virology. 2013 November ; 446(0): 283–292. doi:10.1016/j.virol.2013.07.037.

Dual-Color HIV Reporters Trace a Population of Latently Infected Cells and Enable Their Purification

Vincenzo Calvanese[1,3], **Leonard Chavez**[1,3], **Timothy Laurent**[2,4], **Sheng Ding**[2,4], and **Eric Verdin**[1,3,*]

[1]Gladstone Institute of Virology and Immunology, 1650 Owens Street, San Francisco, CA 94158

[2]Gladstone Institute of Cardiovascular Disease, 1650 Owens Street, San Francisco, CA 94158

[3]Department of Medicine, University of California, San Francisco

[4]Department of Pharmaceutical Chemistry, University of California, San Francisco

SUMMARY

HIV latency constitutes the main barrier for clearing HIV infection from patients. Our inability to recognize and isolate latently infected cells hinders the study of latent HIV. We engineered two HIV-based viral reporters expressing different fluorescent markers: one HIV promoter-dependent marker for productive HIV infection, and a second marker under a constitutive promoter independent of HIV promoter activity. Infection of cells with these viruses allows the identification and separation of latently-infected cells from uninfected and productively infected cells. These reporters are sufficiently sensitive and robust for high-throughput screening to identify drugs that reactivate latent HIV. These reporters can be used in primary CD4 T lymphocytes and reveal a rare population of latently infected cells responsive to physiological stimuli. In summary, our HIV-1 reporters enable visualization and purification of latent cell populations and open up new perspectives for studies of latent HIV infection.

INTRODUCTION

The discovery of effective therapies against HIV, called highly active antiretroviral therapy (HAART), has transformed a once deadly disease into a life-long chronic condition (Palella et al., 1998). By hijacking the viral machinery during infection, HAART effectively reduces infection to undetectable levels. Nonetheless, complete suppression of viral replication by HAART cannot clear HIV infection and the virus reappears rapidly upon treatment interruption (Richman et al., 2009). HIV persists under HAART in a rare population of long-lived, latently infected cells. In addition, the persistence of latent reservoirs feeds an inflammatory-like state that contributes to the development of accelerated aging phenotypes and accompanying age-related diseases in the HAART-treated HIV-positive population (Deeks, 2011).

Correspondence: Eric Verdin, MD, Gladstone Institute of Virology and Immunology, 1650 Owens Street, San Francisco, CA 94158, (415) 734-2000, eric.verdin@gladstone.ucsf.edu.

HIV latency is defined as a state in which proviral DNA is integrated irreversibly in the cell genome, but expression of the viral genes is silenced due to a repressed state of the viral LTR promoter (Hakre et al., 2011). Alternatively, HIV latency can be due to blockade of virus production at any step (Colin and Van Lint, 2009).

Latently-infected cells are extremely rare in patients and carry silent integrated HIV genomes that produce no detectable virus. Current technologies do not allow the identification and purification of live infected cells that do not express any HIV proteins. Latency has therefore been studied “a posteriori” via reactivation of expression of the latent provirus. This type of analysis has allowed the quantification of latent cells in different lymphoid populations and the testing of different drugs that reactivate latent HIV. However, our inability to identify latently infected cells before reactivation has precluded a full understanding of the latency process.

In this study, we present a novel tool that uses fluorescent reporter–based HIV constructs expressing two fluorescent proteins, one dependent and one independent of HIV promoter activation state. This reporter system allows the detection and purification of a cell population of latently infected cells that can be reactivated by physiological and pharmacological stimulation. We show that this system can be used in various cell lines to identify and purify polyclonal populations of latently infected cells. Such populations can be used in high-throughput assays while overcoming the clonal-derived biases of current *in vitro* systems. We also show that these viral constructs are suitable for the study of latency in human primary $CD4^+$ T cells.

RESULTS

Dual-Color Viruses Allow Direct Labeling of Live HIV Latently Infected Cells

To identify latently infected cells prior to reactivation, we designed two HIV-1-based lentiviral constructs in which LTR expression is monitored by production of a fluorescent protein while another independent transcriptional unit expresses a spectrally distinct fluorescent protein under the control of an independent promoter. To construct the first clone, we used the 89.6/DNE/SFG reporter in which *nef* is replaced by a Spleen Focus Forming Virus (SFFV)-promoter-driven enhanced green fluorescent protein (EGFP; Fig. 1B) (Carter et al., 2010). This clone has an *env* deletion, which limits infection to a single round. We used a sequence- and ligation-independent cloning (SLIC) (Li and Elledge, 2012) strategy to reconstitute the *nef* ATG sequence and replace the remainder of the *nef* open reading frame with the sequence of a red fluorescent protein, mApple (Shaner et al., 2008) (Fig. 1B, D); this construct was named 89.6/DNE/mApple/SFG (89mASG).

The second construct was derived from the HXB2-based R7/3 clone bearing EGFP in place of *nef* and an *env* deletion (Jordan et al., 2003) (Fig. 1C). We used the SLIC technique to insert the whole EF1α-mCherry transcriptional unit between the EGFP and the virus 3′ LTR (Fig. 1C, D). We named this construct R7/E-/GFP/EF1a-mCherry (R7GEmC).

To test the potential of these viral reporters to differentiate latent from actively infected and uninfected cell populations, we infected Jurkat T cells with our new constructs (Fig. 1E, F).

After infection, a double-positive population expressing the HIV promoter-dependent reporter and the HIV promoter-independent reporter (SFFV or EF1α promoter) emerged for both viruses (Fig 1E, F). In addition, we detected a single-positive population expressing only the HIV promoter-independent reporter, green for 89mASG (Fig. 1E) and red for R7GEmC (Fig. 1F).

To confirm that the single-positive cells expressing only the non-HIV promoter-driven reporter were latently infected cells, we sorted the GFP-only-positive and mCherry-only-positive cells from the 89mASG-infected and R7GEmC-infected pools, respectively, as well as the double-positive (productively infected) and the double-negative (uninfected) cells for each pool (Fig. 1G, H; left). The single-positive and double-negative cells were expanded *in vitro* after sorting, whereas the double-positive cells did not expand efficiently and largely died after sorting (especially the 89mASG-infected; not shown), as predicted by the cytotoxic properties of active viral infection (Cummins and Badley, 2010). The different sorted populations were analyzed for viral DNA, RNA and protein content. Whereas the double-negative cells had low HIV DNA levels, the single-positive cells had DNA amounts comparable to those of double-positive cells (Fig. 1I) but expressed no detectable viral mRNA (Fig. 1J) or protein (Fig. 1K). Only the double-positive population expressed viral transcripts and proteins. These results are consistent with our model that cells expressing only the non-HIV promoter-driven reporter were latently infected cells

Cells Enriched for HIV-Promoter Independent Expression Contains an HIV Genome That Can Be Reactivated

To estimate the fraction of single-positive cells that can be reactivated in terms of HIV expression, we treated the purified cells with drugs reported to reactivate latent HIV, including tumor necrosis factor (TNF)–α (Jordan et al., 2003); prostratin, a protein kinase C (PKC) activator (Williams et al., 2004); and suberoylanilide hydroxamic acid (SAHA) (Contreras et al., 2009), a non selective histone deacetylase (HDAC) inhibitor. All drugs increased expression of HIV promoter-dependent reporter (Fig. 2A, B top, C, D). Testing of drug combinations that act on different pathways showed maximal reactivation in response to combined SAHA and prostratin treatment, as previously reported by others (Reuse et al., 2009). In both 89mASG- and R7GEmC-infected latent populations, we observed spontaneous reactivation of latency in the absence of activating molecule, likely reflecting the bi-stable nature of HIV expression (Weinberger et al., 2008).

Due to the integration site of the provirus or the cell state, it is possible that some latently infected cells were classified as double negative because of silencing of both the HIV promoter and the SFFV or EF1α promoter. To address this possibility, we treated the double-negative populations with the same drugs (Fig. 2A and B, bottom) and found only very limited reactivation, affecting <1% of the population. This implies that the silent HIV provirus in the double-negative population has little to no ability to reactivate in response to stimulation of latent HIV-reactivating cell pathways.

This two-color latency model, which relies on *de novo* cell infection, can easily be transferred to study the biology of latency in a wide variety of cell types. As an example, we infected and sorted two additional T-cell lines commonly used in HIV biology, SupT1 (Fig.

2E) and A301 (Fig. 2F). Comparison of the sorted latent populations from those cell lines and Jurkat T cells with an extensive panel of HIV-reactivating drugs—including TNFα, prostratin, SAHA, phorbol myristate acetate (PMA), bryostatin, hexamethylbisacetamide (HMBA), and phytohemagglutinin type-M (PHA-M)(Fig. 2G)—revealed significant differences in drug-independent and drug-dependent reactivation rates. This observation supports the concept that use of a non-clonal, non-stimulus-biased experimental system to study HIV latency, as exemplified by these new viruses, adds significance and robustness to the study of mechanisms for reactivation from latency.

Two-Color HIV Latency Model Can Be Used For High-Throughput Screening

Next, we tested the power of this novel HIV latency experimental system to identify novel drugs that reactivate latent HIV in a high-throughput format. We plated 5,000 GFP-only-positive cells of 89mASG-infected Jurkat T cells in each well of 384-well plates, coated with a protein solution (Cell-tak) to induce cell attachment and efficient imaging. Preliminary experiments indicated that this protocol yielded the lowest background reactivation and the highest dynamic range (up to 75% cell reactivation with the most effective drug combinations) (data not shown). Cells were treated with 1,120 individual compounds from the Tocriscreen biologically active compound library at 30 μM for 24 hr (drug combinations are shown in Fig. 2A, B) before they were stained with Hoechst. Next, we imaged each well and quantified total red fluorescence (indicative of reactivated virus) and total blue fluorescence (Hoechst-stained nuclei) (Fig. 3A).

For most compounds in each plate, we found a uniform distribution of signal around the median of the negative controls, while a notably higher red signal for positive controls that were added in control wells on each plate (TNF, SAHA, Prostratin and their combinations as described in the previous section) (Fig. 3A). We also identified a group of drugs that reactivated latent HIV, although to a lesser extent than the positive controls SAHA and prostratin (Suppl. Table 1). Some, such as resveratrol (Krishnan and Zeichner, 2004), and genistein (Gozlan et al., 1998), have been reported previously to reactivate latent HIV, thereby validating this experimental system. In addition, a number of unanticipated and novel drug classes emerged from the analysis, such as those that act on epidermal growth factor receptor (EGFR), dopamine and serotonin receptors.

Next, using the 89mASG and R7GEmC constructs and FACS analysis, we further tested a small group of commercially available drugs and analogs not present in the Tocris library that act on similar pathways, to assess their involvement in HIV latency maintenance. Cells were treated with the dopamine receptor agonist apomorphine, used clinically as an emetic and for male impotence, and the D2-receptor-specific analog R-(−)-propylnorapomorphine. In addition, we tested the serotonin receptor antagonists ritanserin and the antipsychotic clozapine, the EGFR receptor antagonists AG555 and AG18 (candidates for specific cancer treatments), the resveratrol analogs piceatannol and pterostilbene (antioxidants with broad and incompletely understood mechanisms of action), the adenosine reuptake inhibitors dilazep and dipyridamole (used as vasodilators and platelet anti-aggregants), the cdc25 dual-phosphatase inhibitor NC95397, the selective BTK inhibitor (−)-terreic acid, and the HMG-CoA synthase inhibitor simvastatin (Fig. 3B, C). Among these, AG555, piceatannol, dilazep

and terreic acid produced slight but significant reactivation activity in the 89mASG (Fig. 3B, C) and R7GEmC (Fig. 3B, D) single-positive latent populations. Other molecules were less effective (simvastatin) or had distinct effects in the two HIV clones (apomorphin). In some cases, the intrinsic fluorescence of the molecule produced clear artifacts or false positives (see NSC 95397; Fig. 3B).

A recent study showed that the approved HDAC inhibitor SAHA can reactivate HIV RNA expression in a subset of patients (Archin et al., 2012). Thus, it might be of interest to identify compounds that can potentiate HIV reactivation by SAHA or prostratin or TNFα. Sorted latent-cell populations were co-treated for 24 h with low levels of SAHA, prostratin and TNFα, and several effective, non-toxic concentrations of the most promising compounds (Fig. 3E). Interestingly, combining SAHA with terreic acid, dilazep or piceatannol (10 μM) strongly enhanced the effect of low SAHA concentrations on HIV latency on these cells; the same drugs were also synergistic with prostratin, as indicated by the fact that their combined activity when present together was greater than the sum of their individual activities. TNFα combinations showed synergistic interaction in most combinations except terreic acid, possibly indicating that the drugs act on the same pathway.

Two-Color HIV Constructs Detect Latency in Primary T Cells

Studies of the basic biology of HIV latency have recently emphasized the use of primary cell–based models in an effort to more closely mimic the situation in patients. The use of primary $CD4^+$ T cells from human donors nonetheless remains a challenge, due to low latency establishment rates and limited expansion potential. Resting peripheral $CD4^+$ T cells are generally refractory to HIV infection and require pre-stimulation to achieve efficient infection. Furthermore, T-cell-receptor stimulation and IL2 and/or IL7 supplementation (Bosque et al., 2011), which is needed for expansion of these cells in culture and for permissive HIV infection, activate the latent HIV provirus, thereby making expansion of latently infected cells unfeasible unless a transformed-like phenotype is induced (Yang et al., 2009).

Despite these limitations, a number of experimental model system for HIV latency have been established in primary CD4+ T cells (Hakre et al., 2012). We therefore tested our viral constructs for their potential to generate a latent infection in primary CD4+ T cells. Cells were activated with anti-CD3 and anti-CD28-coated dynabeads for 48 hours and infected with both viruses. We found that both viruses infected activated $CD4^+$ T cells efficiently, generating an active infection as determined by expression of the HIV promoter-dependent reporters mApple (for 89mASG)(Suppl. Fig. 1), and GFP (for R7GEmC)(Fig. 4A, B). A very small population of cells expressing only the latency-associated fluorescent marker was also generated in approximately 1 of 100 active infection events. As the GFP signal in 89mASG-infected primary cells was dim and difficult to distinguish from uninfected cells, the R7GEmC construct was used for additional experiments in primary CD4+ cells.

We measured HIV proviral DNA and HIV gag in sorted mCherry-only populations compared to uninfected and actively infected sorted populations. Viral DNA was detected at high levels in double-positive cells and slightly lower levels in mCherry-positive cells (Fig. 4C). Interestingly, lower but still detectable amounts of proviral DNA were also detected in

double-negative cells, indicating that some latent events might be found in this population if EF1α promoter expression is also blocked. As predicted, the HIV *gag* protein was also detectable in the actively infected population, and absent in latent and uninfected populations (Fig. 4D).

We next evaluated the extent to which mCherry-only-positive populations could be reactivated by further stimulation. After sorting the three populations of mCherry-only-expressing, GFP-positive, and double-negative cells, cells were treated with anti-CD3/28-coated beads to reactivate the latent provirus (Fig. 4E). The latent population responded to this treatment with a 15–18% increase in cells expressing GFP. The double-negative population also responded to a lesser extent, with 0.5–2% reactivation. A population of very bright mCherry-only cells did not respond to treatment, suggesting aberrant integration events or non-reactivatable latent provirus. A subset of less-bright mCherry-only positive cells also responded to prostratin and SAHA treatment (Fig. 4F), suggesting that this population of primary $CD4^+$ T cells contains latently infected, reactivatable cells.

HIV latency *in vivo* is reported to result, in part, from pre-integration latency, whereby unintegrated proviral DNA (after full retrotranscription) is maintained in a stable cytoplasmic form in a quiescent cell, and can respond to cell activation by *de novo* integration and productive infection (Pierson et al., 2002). To rule out pre-integration latency, we infected activated $CD4^+$ T cells with R7GEmC in the presence of the HIV integrase inhibitor raltegravir (Suppl. Fig. 2A). Under these conditions, we found no integration-independent expression of the fluorescent proteins after 3 days, thereby excluding pre-integration latency as a major mechanism in this primary-cell-infection model. In addition, raltegravir treatment did not reduce viral reactivation in the mCherry-only-positive population, indicating that all reactivatable latent cells were in a post-integration latency stage (Suppl. Fig. 2B).

DISCUSSION

A major obstacle in the development of an eradication-based cure for HIV is the virus' ability to establish latent infection (Trono et al., 2010). As latent viruses are inactive and extremely rare *in vivo*, the ability to detect and enrich for a latently infected cell population would powerfully advance our understanding of the mechanism of HIV latency. Here, we describe two HIV-reporter systems that allow for the identification and purification of live, latently infected cells and their separation from actively infected and uninfected cells.

Using Jurkat and other cell lines, we show that purification of latently infected cells from a primary infected pool allows for the study of HIV latency independent of cell clonality, insertion sites in the genome, and reactivating stimuli. The dynamic range of reactivation assays is also increased, due to the separation of homogeneous latently infected from uninfected cells. This permits the detection of novel compounds that reactivate latent HIV, providing new possibilities for combination therapies.

A recent paper has reported a similar dual fluorescence HIV construct to study HIV latency. In this construct, a GFP marker was inserted in the Gag gene leading to the synthesis and

incorporation of a fusion Gag-GFP protein which is proteolytically released in the mature virion and used to monitor HIV expression. A CMV-mCherry cassette was added in place of nef to monitor integration events (Dahabieh et al., 2013). This tool has similar applications to the HIV reporter that we describe in this work, although the presence of GFP in the virion limits the possibility of studying the early kinetics of integration and HIV promoter activation. In addition, the use of the CMV promoter which shows variable activity in hematopoietic lineages and a high dependence on the degree of CD4+ T cell activation, might not be optimal (Sirven et al., 2001).

Other current cell models that involve enrichment of latently infected cells require prestimulation with specific compounds or cytokines to identify the infected population, and subsequent induction of a latent state (Bosque and Planelles, 2009; Duverger et al., 2012; Hakre et al., 2012). This experimental system skews the study of latent HIV populations by restricting analysis to a subset of latent infection events responsive to that compound and able to overcome the cytotoxic effect of HIV reactivation. Our constructs detect a population of latently infected cells regardless of their responsiveness to the reactivation of cellular pathways, and thus more closely approximates the establishment of latent infection early in the viral life cycle prior to initiation of *tat*-dependent HIV transcription.

Although our system overcomes the issues of clonality and dependence on specific reactivation pathways, it does not detect latent infection events that repress both the HIV and the EF1α or SFFV promoters. Although this limitation could potentially skew analysis of latent infection events, we detect lower levels of proviral DNA in the double-negative population than in the fluorescent cells, indicating that the events that we missed are relatively rare. In addition, a very small number of the potentially latently infected cells in this population are responsive to pharmacological reactivation, which implies that these double-negative latent cells are incapable of, or refractory to, rebound of the viral life cycle and may represents HIV proviruses that are terminally silenced. In contrast, Dahabieh *et al.* observe a significant and robust of reactivation from latency in the sorted double negative population, possibly due to a subset of latent events in their system that fails to activate the CMV promoter (Dahabieh et al., 2013).

Our HIV latency model uses a replication-deficient lentiviral system that is easily pseudo-typed and packaged in a number of ways, which facilitates its use for the study of latent infection events in any cell population of interest. Our study focused on the widely used Jurkat T–cell line; however, two other T cell–derived cell lines, A301 and SupT1, can also be infected if the receptors and co-receptors expressed are compatible with the viral envelope of choice (in our experiments, a dual-tropic HIV gp160 derived from a patient isolate (clone 92HT593.1) (Gao et al., 1996). Our system can thus be potentially used in different cell types and candidate reservoirs of the latent HIV pool.

The use of two viral clones on different cell lines allowed us to observe a phenomenon of variable basal reactivation from latency in the isolated latently infected populations. The vector R7GEmC appears to have higher basal reactivation, which leads to a tendency to double positive cell accumulation upon re-expansion from sorted mCherry-only cells. This basal reactivation as well as the responsiveness to different drugs also varied among the

three tested cell lines. This instability might be a result of selecting latent infection events early after infection, before lon-gterm maintenance processes have established, and might reflect the bistable nature of HIV transcription, as described by Weinberger et al. (Weinberger et al., 2008).

The use of two viral clones on different cell lines allowed us to observe a phenomenon of variable basal reactivation from latency in the isolated latently infected populations. The vector R7GEmC appears to have higher basal reactivation, which leads to a tendency to double positive cell accumulation upon re-expansion from sorted mCherry-only cells. This basal reactivation as well as the responsiveness to different drugs also varied among the three tested cell lines. This instability might be a result of selecting latent infection events early after infection, before longterm maintenance processes have established, and might reflect the bistable nature of HIV transcription, as described by Weinberger et al. (Weinberger et al., 2008).

To demonstrate the potential of these dual-color viruses for high-throughput applications such as drug discovery, we conducted a small-scale high-throughput screen of constructs with a biologically active compound library. Although none of the 1,120 compounds tested showed higher reactivation potential than the known latent HIV reactivators, we identified classes of clinically or experimentally used drugs, not typically associated with the biology of HIV latency, that produced small but significant reactivation of the provirus, such as drugs acting on neurotransmitter receptors or Tyr kinases. In flow cytometry assays of the sorted latent-cell population, some of the identified drugs showed a dose-dependent reactivation of latency; in combination with low doses of the current leads for latent HIV reactivation (SAHA, prostratin) they also revealed a synergistic effect that might be exploited for research and as a therapeutic tool in current and future clinical protocols.

For a preliminary validation in primary cells, we tested the HIV latency model in activated $CD4^+$ T cells. These cells contain the main constituents of the latent HIV reservoir, such as central and transitional memory $CD4^+$ T cells. As reported (Baldauf et al., 2012), resting $CD4^+$ T cells are refractory to HIV infection, with few or no fluorescent cells when viruses are tested in freshly isolated populations (not shown). Although we prestimulated cells with anti-CD3/CD28-coated beads to boost infection levels, latent infection rates remained very low, as is predicted for a fully activated T cell. The mApple-only-expressing cells obtained from infection of primary activated CD4+ cells had proviral DNA levels similar to those of the double-positive population, but did not express viral products such as p24. Only a small but measurable part of the mApple-only population (<20%) responded to αCD3/CD28 stimulation or to molecules that reactivate latent HIV in other systems (SAHA, Prostratin). Importantly, we can detect a small population of latently infected, reactivatable CD4+ T cells after infection of activated T cells.

In conclusion, we present a powerful instrument to study HIV latent infection. These new reporter viruses offer the advantage of enabling detection and purification of live, latent-HIV-infected cells and to study the kinetics of latency establishment early upon cell infection. This tool can further advance the study of HIV latency and provide new routes to accelerate the quest for a functional cure and eradication of HIV infection.

EXPERIMENTAL PROCEDURES

Plasmid Construction

HIV clones 89.6-DNE-SFG (donated by Dr. Kathleen Collins's laboratory) and R7/E-/GFP were linearized by PCR using opposing primers (see Suppl. table 2, #A and B) in the position selected for insertion (Fig. 1). mApple and the EF1a-mCherry sequences were cloned in the respective plasmids by a modified SLIC technique (Li and Elledge, 2012). Briefly, inserts were PCR-amplified from plasmid templates with primers that have a 20 bp 5′-overhang complementary to the end sequences of the blunted plasmids (see Suppl. table 2, #C and D). DNA from all amplifications was gel-purified, digested with 3′-5′ exonuclease (T4-polymerase, Novagen, 30 min, 25°C) and heat-inactivated (20 min, 75°C). Digested inserts and vectors for each construct were mixed at a 2:1 molar ratio for complementary-end sequence annealing (20 min, 37°C) and transformed in chemically competent Stbl-2 *E. coli* (Life Technologies). Positive clones were resequenced entirely.

Virus Production

HEK293T cells were cotransfected with the viral plasmid clone of interest and the *env*-encoding plasmid pSVIII-92HT593.1 (NARP), using Lipofectamine 2000 (Invitrogen). Medium (DMEM, 10% FBS) was changed 8 h post-transfection and collected at 72 h. Virus supernatant was filtered through a 0.45 μm-pore membrane, concentrated by ultracentrifugation and stored at −80°C. Virus concentration was estimated by p24 titration (HIV-1 alliance p24 ELISA kit, PerkinElmer).

Cells and Treatments

HEK293T, Jurkat, A301 and SupT1 cell lines were obtained from ATCC. Suspension cells were cultured in RPMI 1640 supplemented with 10% FBS, 100 U/ml penicillin, 100 mg/ml streptomycin and 2 mM L-glutamine (PSG) (37°C, 5% CO_2). Peripheral blood from healthy human donors was obtained from the Stanford Blood Center and processed the day of collection. $CD4^+$ T cells were isolated with RosetteSep Human $CD4^+$ T-Cell Enrichment Cocktail (Stem Cell Technologies) and cultured in human cell medium (HCM, RPMI, 10% human AB pooled serum, PSG). Resting $CD4^+$ T cells were activated in U-bottom 96-well TC plates with 25 μl human anti-CD3 and anti-CD28-coated dynabeads (Life technologies)/10^6 cells (48 h). Dynabeads were removed by magnetic separation and cells seeded in HCM with 30 IU/ml rhIL-2 (NIH AIDS Reagents Program). Cell lines and activated $CD4^+$ cells were infected by spinoculation (Lassen et al., 2012) with a virus amount equivalent to 20 ng p24 or as indicated. Viral infection was assessed by FACS analysis after 72 h. At 5 days post-infection, cells were sorted to separate negative, single- or double-positive cells. Sorted cell lines were treated after re-expansion for 5–15 days. Cells were seeded in 96-well U plates and treated for 24 h before analysis. $CD4^+$ T cells were reseeded after sorting in 96-well U plates with HCM in the absence of IL-2 and treated after 24 h with drugs or human T-activator Dynabeads (48 h). Raltegravir (NARP), TNF-α (LT), prostratin, SAHA, bryostatin-1, PMA, HMBA, PHA-M (all from Sigma) were used in culture at indicated concentrations. This study was conducted according to the principles expressed in the Declaration of Helsinki. All individuals provided written informed consent

for the collection of samples and subsequent analysis, as approved by the Institutional Review Board of the Stanford University Blood Bank.

Flow Cytometry and Cell Sorting

EGFP, mApple and mCherry fluorescence were measured in a MACSQuant VYB FACS analyzer (Miltenyi Biotech GmbH), FACSCalibur, LSRII, and sorted in a FACSAriaII (all BD). Data were analyzed using FlowJo 9.4 (TreeStar).

DNA, RNA and Protein Extraction, qPCR and Western Blot

DNA and RNA were extracted with Dneasy and RNeasy kits, respectively (Qiagen). RNA was retrotranscribed with the high capacity kit cDNA (Life technologies) and qPCR was performed in the AB 7900HT Fast Real-Time PCR System, using TaqMan 2x Master Mix and the appropriate primer-probe combinations (Suppl Table 2, #E, F, and G). Quantification for each qPCR reaction was assessed by interpolation on a template dilution curve. As normalization controls TaqMan Copy Number Reference Assay, RNase P was used for genomic DNA and TaqMan assay GAPDH Hs99999905_m1 for cDNA. Protein was extracted from freshly sorted cells in RIPA buffer, followed by SDS-PAGE. Bands were detected by chemiluminescence (ECL Hyperfilm Amersham) or fluorescence (Licor Odyssey) detection with anti-vif, HIV-p24 and -α-actin (Sigma) primary antibodies.

Fluorescence Microscopy

Cells were analyzed with an Axio observer Z1 microscope (Zeiss) equipped with EC Plan Neofluar 20X/0.5 PHM27, EC Plan Neofluar 40X/0.75 PH, and Plan Apo 63X/1.4 Oil DIC M27 objectives, filter sets 38HE, 43HE, 45, and 50, Optovar 1.25X and 1.6X magnification, and an Axiocam MRM REV 3.

Drug Screening

Sorted GFP-only 89mASG cells-infected Jurkat cells were expanded in culture and seeded at a 5 × 103 cells/well density in 384-well plates (black, clear bottom, Greiner), coated with Cell-Tak (BD). Tocriscreen total drug screening library, containing 1120 biologically active compounds dissolved in DMSO, was dispensed in the plate at a concentration of 30 μM, using the automated Beckman and Coulter Biomek FXP robot and 50 nl VP 384 pin tool. After 24h culture in standard conditions, Hoechst 33342 was automatically dispensed with Thermo multodrop 384 to each well to evaluate total cell number of cell; plates were imaged in the InCell analyzer and analyzed with InCell Developer image analysis software. We quantified the total area masked by the nuclear stain and the total area of cells expressing mApple as proxies for cell number and number of cells which had reactivated viral transcription, respectively. On negative control wells, we calculated the median and standard deviation and used these statistics to select significant conditions that differed from these expected values by more than 2SD.

Supplementary Material

Refer to Web version on PubMed Central for supplementary material.

Acknowledgments

We thank Gary Howard for editorial assistance, John Carroll and Teresa Roberts for graphics and Veronica Fonseca for administrative assistance. Eric Verdin is supported by NIDA Avant-Garde-1DP1 DA031126, 1R01 DA030216-01, and is a member of the CARE collaboratory (UNC/NIH–Federal-5-31532).

References

Archin NM, Liberty AL, Kashuba AD, Choudhary SK, Kuruc JD, Crooks AM, Parker DC, Anderson EM, Kearney MF, Strain MC, et al. Administration of vorinostat disrupts HIV-1 latency in patients on antiretroviral therapy. Nature. 2012; 487:482–485. [PubMed: 22837004]

Baldauf HM, Pan X, Erikson E, Schmidt S, Daddacha W, Burggraf M, Schenkova K, Ambiel I, Wabnitz G, Gramberg T, et al. SAMHD1 restricts HIV-1 infection in resting CD4(+) T cells. Nat Med. 2012; 18:1682–1687. [PubMed: 22972397]

Bosque A, Famiglietti M, Weyrich AS, Goulston C, Planelles V. Homeostatic proliferation fails to efficiently reactivate HIV-1 latently infected central memory CD4+ T cells. PLoS Pathog. 2011; 7:e1002288. [PubMed: 21998586]

Bosque A, Planelles V. Induction of HIV-1 latency and reactivation in primary memory CD4+ T cells. Blood. 2009; 113:58–65. [PubMed: 18849485]

Carter CC, Onafuwa-Nuga A, McNamara LA, Riddell Jt, Bixby D, Savona MR, Collins KL. HIV-1 infects multipotent progenitor cells causing cell death and establishing latent cellular reservoirs. Nat Med. 2010; 16:446–451. [PubMed: 20208541]

Colin L, Van Lint C. Molecular control of HIV-1 postintegration latency: implications for the development of new therapeutic strategies. Retrovirology. 2009; 6:111. [PubMed: 19961595]

Contreras X, Schweneker M, Chen CS, McCune JM, Deeks SG, Martin J, Peterlin BM. Suberoylanilide hydroxamic acid reactivates HIV from latently infected cells. J Biol Chem. 2009; 284:6782–6789. [PubMed: 19136668]

Cummins NW, Badley AD. Mechanisms of HIV-associated lymphocyte apoptosis: 2010. Cell Death Dis. 2010; 1:e99. [PubMed: 21368875]

Dahabieh MS, Ooms M, Simon V, Sadowski I. A doubly fluorescent HIV-1 reporter shows that the majority of integrated HIV-1 is latent shortly after infection. J Virol. 2013; 87:4716–4727. [PubMed: 23408629]

Deeks SG. HIV infection, inflammation, immunosenescence, and aging. Annu Rev Med. 2011; 62:141–155. [PubMed: 21090961]

Duverger A, Wolschendorf F, Zhang M, Wagner F, Hatcher B, Jones J, Cron RQ, van der Sluis RM, Jeeninga RE, Berkhout B, Kutsch O. An AP-1 binding site in the enhancer/core element of the HIV-1 promoter controls the ability of HIV-1 to establish latent infection. J Virol. 2012

Gao F, Morrison SG, Robertson DL, Thornton CL, Craig S, Karlsson G, Sodroski J, Morgado M, Galvao-Castro B, von Briesen H, et al. Molecular cloning and analysis of functional envelope genes from human immunodeficiency virus type 1 sequence subtypes A through G. The WHO and NIAID Networks for HIV Isolation and Characterization. J Virol. 1996; 70:1651–1667. [PubMed: 8627686]

Gozlan J, Lathey JL, Spector SA. Human immunodeficiency virus type 1 induction mediated by genistein is linked to cell cycle arrest in G2. J Virol. 1998; 72:8174–8180. [PubMed: 9733859]

Hakre S, Chavez L, Shirakawa K, Verdin E. Epigenetic regulation of HIV latency. Curr Opin HIV AIDS. 2011; 6:19–24. [PubMed: 21242889]

Hakre S, Chavez L, Shirakawa K, Verdin E. HIV latency: experimental systems and molecular models. FEMS Microbiol Rev. 2012; 36:706–716. [PubMed: 22372374]

Jordan A, Bisgrove D, Verdin E. HIV reproducibly establishes a latent infection after acute infection of T cells in vitro. EMBO J. 2003; 22:1868–1877. [PubMed: 12682019]

Krishnan V, Zeichner SL. Host cell gene expression during human immunodeficiency virus type 1 latency and reactivation and effects of targeting genes that are differentially expressed in viral latency. J Virol. 2004; 78:9458–9473. [PubMed: 15308739]

Lassen KG, Hebbeler AM, Bhattacharyya D, Lobritz MA, Greene WC. A flexible model of HIV-1 latency permitting evaluation of many primary CD4 T-cell reservoirs. PLoS One. 2012; 7:e30176. [PubMed: 22291913]

Li MZ, Elledge SJ. SLIC: a method for sequence- and ligation-independent cloning. Methods Mol Biol. 2012; 852:51–59. [PubMed: 22328425]

Palella FJ Jr, Delaney KM, Moorman AC, Loveless MO, Fuhrer J, Satten GA, Aschman DJ, Holmberg SD. Declining morbidity and mortality among patients with advanced human immunodeficiency virus infection. HIV Outpatient Study Investigators. N Engl J Med. 1998; 338:853–860. [PubMed: 9516219]

Pierson TC, Zhou Y, Kieffer TL, Ruff CT, Buck C, Siliciano RF. Molecular characterization of preintegration latency in human immunodeficiency virus type 1 infection. J Virol. 2002; 76:8518–8531. [PubMed: 12163571]

Reuse S, Calao M, Kabeya K, Guiguen A, Gatot JS, Quivy V, Vanhulle C, Lamine A, Vaira D, Demonte D, et al. Synergistic activation of HIV-1 expression by deacetylase inhibitors and prostratin: implications for treatment of latent infection. PLoS One. 2009; 4:e6093. [PubMed: 19564922]

Richman DD, Margolis DM, Delaney M, Greene WC, Hazuda D, Pomerantz RJ. The challenge of finding a cure for HIV infection. Science. 2009; 323:1304–1307. [PubMed: 19265012]

Shaner NC, Lin MZ, McKeown MR, Steinbach PA, Hazelwood KL, Davidson MW, Tsien RY. Improving the photostability of bright monomeric orange and red fluorescent proteins. Nat Methods. 2008; 5:545–551. [PubMed: 18454154]

Sirven A, Ravet E, Charneau P, Zennou V, Coulombel L, Guetard D, Pflumio F, Dubart-Kupperschmitt A. Enhanced transgene expression in cord blood CD34(+)-derived hematopoietic cells, including developing T cells and NOD/SCID mouse repopulating cells, following transduction with modified trip lentiviral vectors. Mol Ther. 2001; 3:438–448. [PubMed: 11319904]

Trono D, Van Lint C, Rouzioux C, Verdin E, Barre-Sinoussi F, Chun TW, Chomont N. HIV persistence and the prospect of long-term drug-free remissions for HIV-infected individuals. Science. 2010; 329:174–180. [PubMed: 20616270]

Weinberger LS, Dar RD, Simpson ML. Transient-mediated fate determination in a transcriptional circuit of HIV. Nat Genet. 2008; 40:466–470. [PubMed: 18344999]

Williams SA, Chen LF, Kwon H, Fenard D, Bisgrove D, Verdin E, Greene WC. Prostratin antagonizes HIV latency by activating NF-kappaB. J Biol Chem. 2004; 279:42008–42017. [PubMed: 15284245]

Yang HC, Xing S, Shan L, O'Connell K, Dinoso J, Shen A, Zhou Y, Shrum CK, Han Y, Liu JO, et al. Small-molecule screening using a human primary cell model of HIV latency identifies compounds that reverse latency without cellular activation. J Clin Invest. 2009; 119:3473–3486. [PubMed: 19805909]

Highlights

- We report two novel HIV-based viral reporters with fluorescent markers
- These new reporters allow the identification and purification of latent, productive and uninfected cells.
- These reporters can be used in high-throughput screens to identify molecules that reactive latent HIV
- These reporter allow the identification of rare latently infected cells in primary $CD4^+$ cells

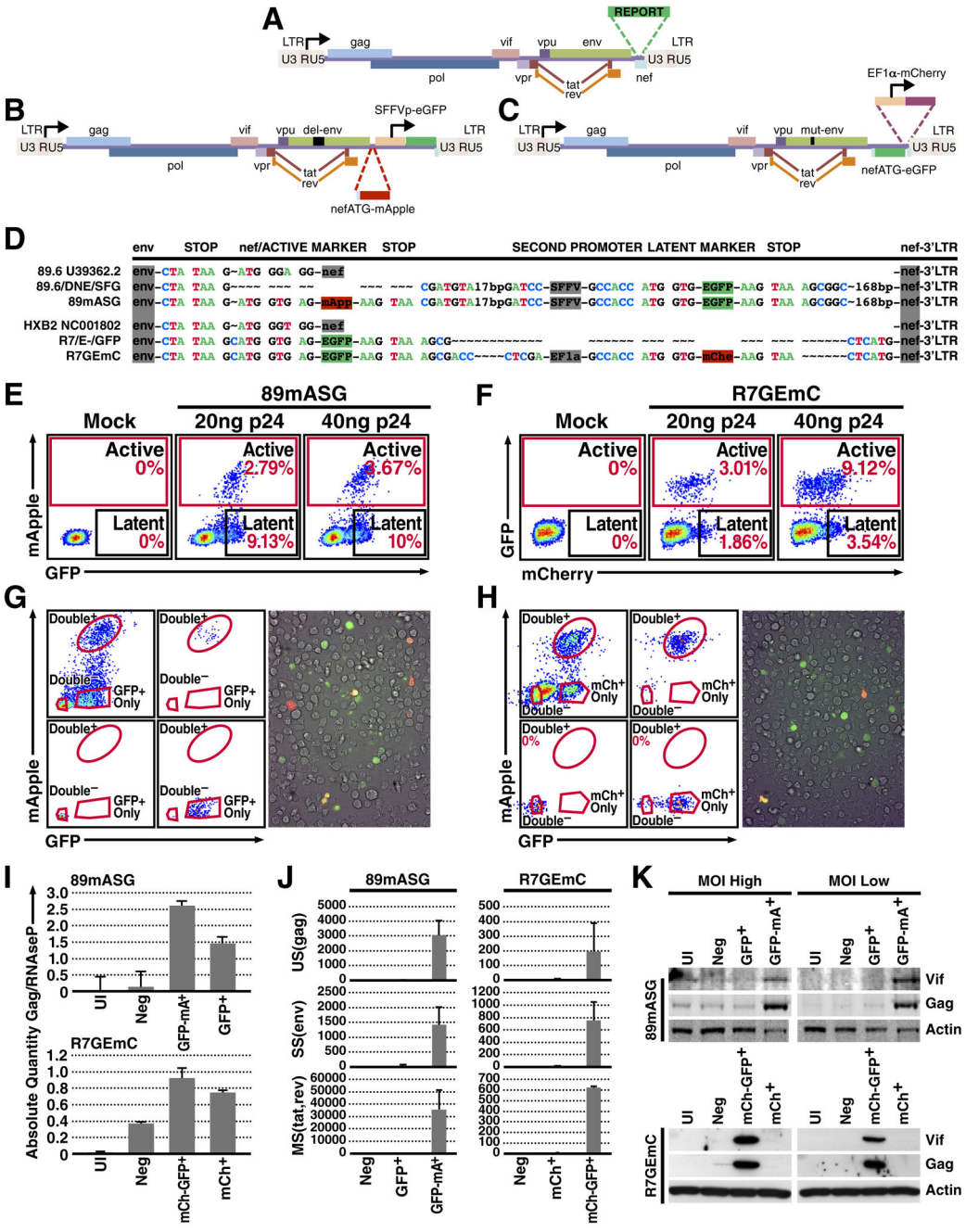

Figure 1. Two-Color Viruses Identify a Population of Latently Infected Cells

(a) Diagram of the derivation of two-color viruses from the original strains, with a scheme of a classical single reporter virus bearing the reporter gene in the *nef* ORF.

(b) In the 89mASG construct, EGFP is under the control of the SFFV promoter and mApple was added upstream of the transcriptional unit in the position of the *nef* ATG (see d).

(c) In the R7GEmC construct, GFP replaces *nef* and a whole transcriptional unit (EF1α-mCherry) was inserted downstream.

(d) Alignment of regions of interest (from the end of *env* to the 3′LTR) of the original 89.6 and HXB2 strains deposited in the NCBI database (U39362.2 and NC001802), the starting

plasmid and final constructs for each of the HIV clones 89mASG (d, top) and R7GEmC (d, bottom). Insertion points of the first reporter in the *nef* ORF, the promoter (SFFV or EF1α, respectively) and the second reporter, followed by the end of *nef* and 5′LTR.

(e,f) Cytometric analysis of Jurkat T cells 3 days post-infection, with the indicated titers of 89mASG (e) and R7GEmC (f).

(g,h) FACS analysis of 89mASG (g, left) and R7GEmC (h, left) Jurkat T cells sorted 5 days post-infection. Double-negative (uninfected), double-positive (actively infected) and single-positive (latently infected, expressing GFP- or mCherry-only) cells are shown for both viral strains. Fluorescence microscopy images of 89mASG- (g, right) and R7GEmC- (h, right) infected Jurkat T cells.

(i) qPCR quantification of proviral DNA in the sorted Jurkat populations, using the primer-probe combination #E for the HIV-1 *gag* gene and *RNAseP* for normalization.

(j) qPCR quantification of viral transcripts of unspliced (US) *gag*, singly- (SS) env and multiply-spliced (MS) tat/rev common regions (#E, F, and G; Suppl. table 2), normalized for cell GAPDH.

(k) Western blot quantification of the HIV proteins vif and gag and the endogenous protein α-actin in the sorted Jurkat populations.

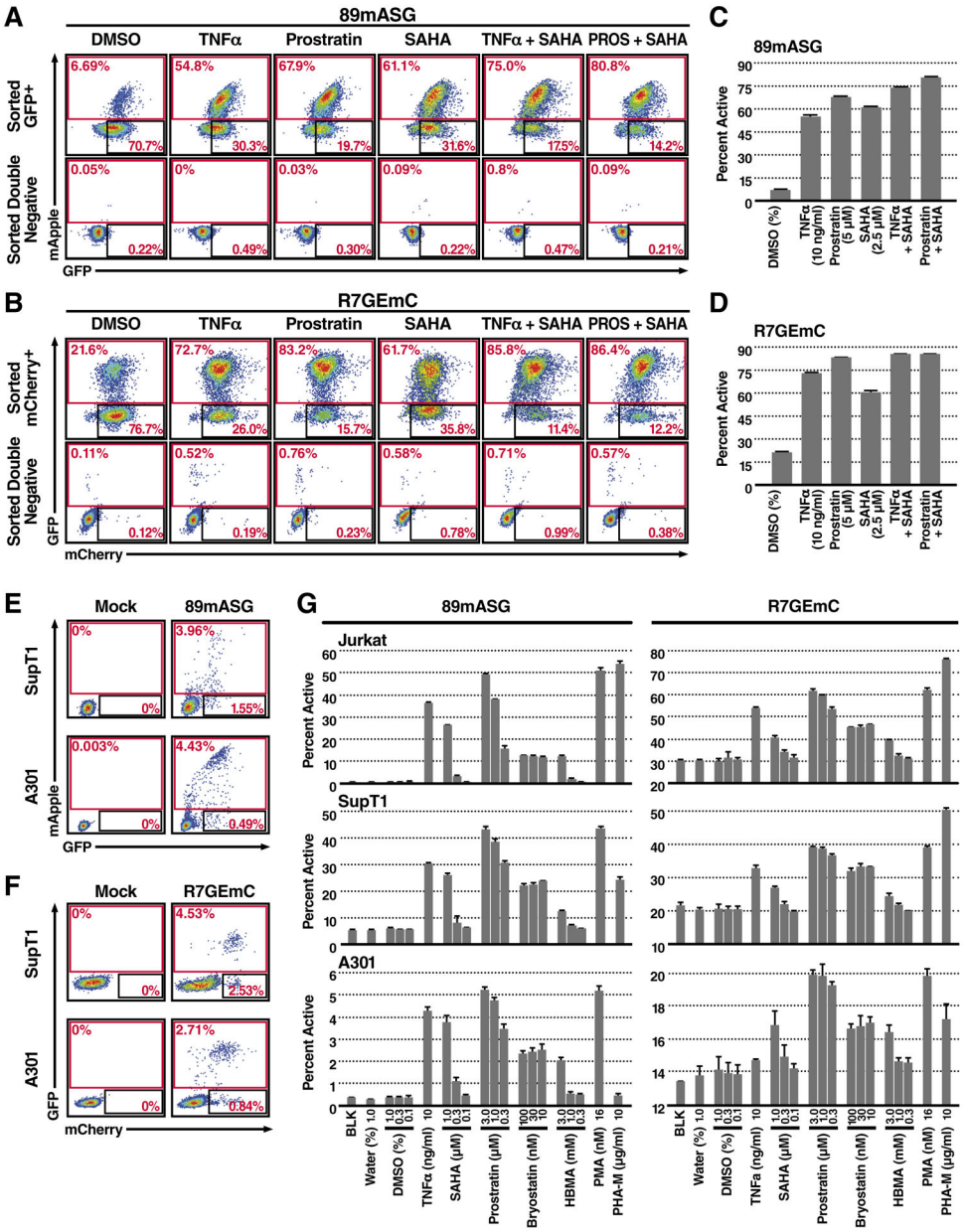

Figure 2. Latently Infected Cells Respond to Reactivating Drugs

(a–d) Five days after sorting, expanded single-positive (latent) and double-negative (uninfected) 89mASG (a, c) and R7GEmC (b, d) Jurkat T cells were treated with 10 ng/ml TNFα, 5 μM prostratin or 2.5 μM SAHA, alone or in combination, as indicated. FACS analysis of a representative treatment (a, b) and histogram quantification of percent population in the active gate for three different experiments (c, d). P<0.001, compared to DMSO control for all treatments. P<0.01 for combination vs. single treatments, except for R7GEmC prostratin vs. prostratin+SAHA P<0.05.

(e,f) FACS analysis of SupT1 and A301 cell lines, infected with 20 ng p24 of 89mASG (e) or R7GEmC (f) virus.

(g) A larger panel of latent HIV-reactivating drugs was used at indicated concentrations on sorted, single positive Jurkat, SupT1 and A301 cells. Histograms show quantification of the percent population in the active gate. Data indicate mean ± SD for three different treatments. $P<0.01$, compared to DMSO 0.1% control for all treatments, except for: SAHA 0.1 not significant (n.s.) in all combinations; SAHA 0.1 n.s. in SupT1 and A301-R7GEmC, $P<0.05$ in Jurkat-R7GEmC; Bryostatin 30 $P<0.05$ in A301-R7GEmC; HMBA 0.3 n.s. in all combinations; HMBA 1 n.s. in A301 and SupT-R7GEmC, $P<0.05$ in Jurkat-R7GEmC and SupT-89mASG; PHA-M n.s in A301-89mASG and $P<0.05$ in A301-R7GEmC.

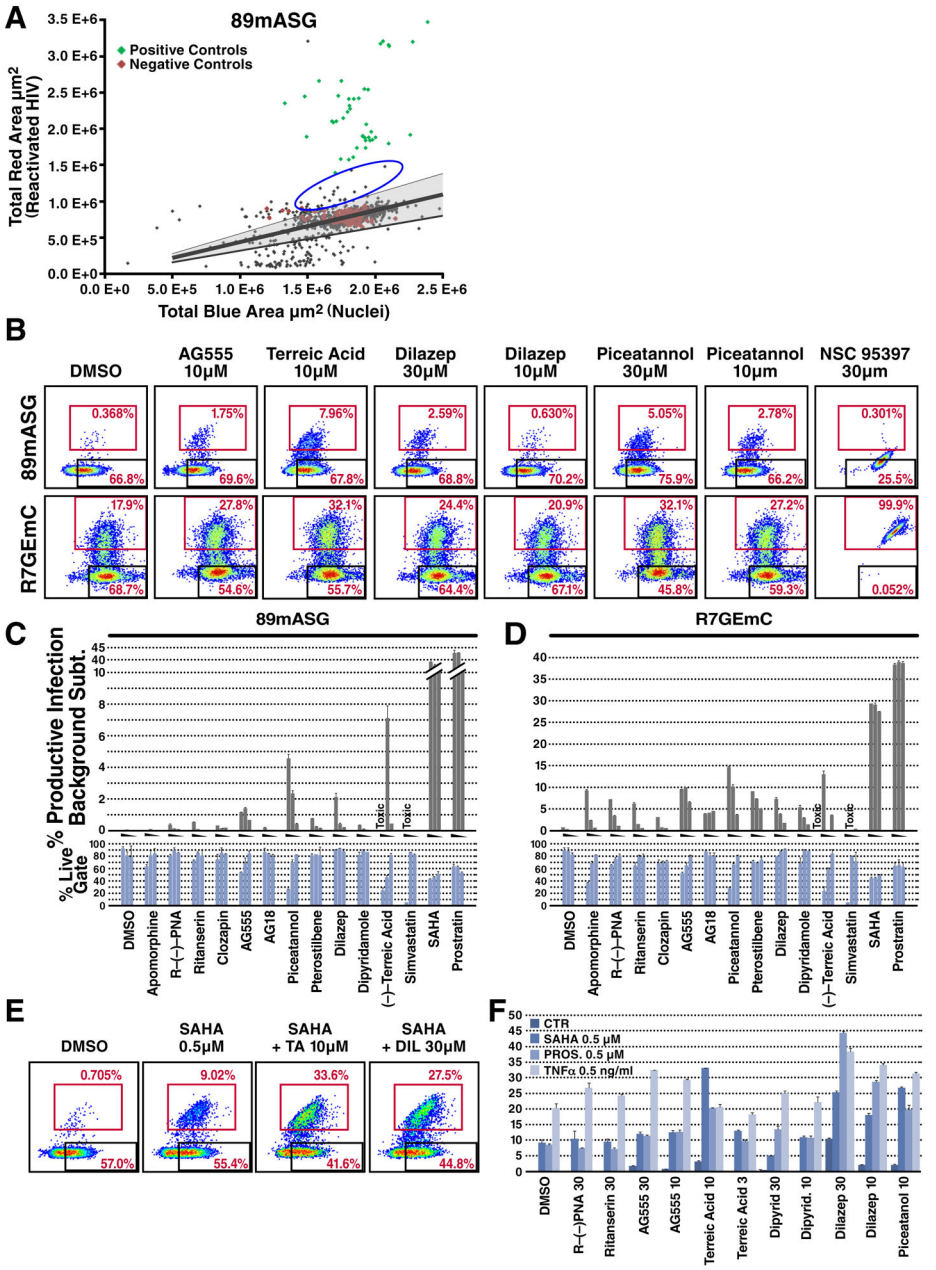

Figure 3. High-Throughput Screening Identifies New Reactivator Drugs Using Two-Color HIV Constructs

Sorted 89mASG-infected, GFP-only-positive Jurkat cells were used to test the Tocriscreen drug library for latent HIV reactivation (see Methods).

(a) Dot plot showing quantification of total blue area (Hoechst 33342 signal, total cell) against total red area (mApple signal, reactivated HIV). Red dots indicate the position of untreated wells; the shaded area indicates the median ± 2SD of the red/blue area ratio for negative control wells. Green dots indicate positive control wells, treated with 10 ng/ml TNFα, 5 µM prostratin or 2.5 µM SAHA and their combinations. Blue circle shows novel reactivators identified in the screening (see Suppl. Table 1).

(b) Validation of representative hits by FACS analysis. Apomorphine and its analog R-(−)-propylnorapomorphine (PNA), ritanserin, clozapin, AG555, AG18, piceatannol, pterostilbene, dilazep, dipyridamole, terreic acid (TA), simvastatin and NSC95397 were used to validate hits and pathways identified by drug screening. Representative FACS plots of sorted single-positive Jurkat T cells for both viruses. The productive gate contains the reactivated cells. In the last plot on the right, NSC95397 treatment shows alteration of the fluorescent profile by the drug fluorescence.

(c,d) Histogram plot of percent population in the productive gate (grey) for each treatment and percentage of cells in the live gate (light blue) for sorted single-positive Jurkat T cells for 89mASG (c) and R7GEmC (d) reporters. Data shown as mean ± SD for three different treatments. For each compound, a grey triangle between the histograms indicates decreasing drug concentration (30, 10 and 3 μM). Treatments for which cell death was predominant are labeled TOXIC. Ritanserin 30μM, clozapin 30μM, AG555 30, 10 and 3μM, piceatannol 30 and 10μM, pterostilbene 30μM, dilazep 30μM, TA 10 and 3μM ($P<0.01$) and PNA 30μM, piceatannol 3μM, pterostilbene 10μM, dipyridamole 30μM ($P<0.05$) show significant reactivation of the latent 89mASG virus compared to the DMSO control. Apomorphin 30μM, PNA 30μM, ritanserin 30μM, clozapin 30μM, AG555 30, 10 and 3μM, AG18 30, 10 and 3μM, piceatannol 30 and 10μM, pterostilbene 30 10 and 3 μM, TA 10μM ($P<0.01$) and PNA 10μM, ritanserin 10μM, piceatannol 3μM, dilazep 30, 10 and 3μM, TA 3μM ($P<0.05$) show significant reactivation of the latent R7GEmC virus compared to the DMSO control.

(e) FACS analysis of drug treatments combined with 0.5 μM SAHA, 0.5 μM prostratin and 0.5 ng/ml TNFα. Representative FACS plots of sorted GFP-only-positive Jurkat T cells for 89mASG treated with DMSO (control), SAHA (0.5 μM) alone or with terreic acid (10 μM) and dilazep (30 μM).

(f) Histogram plot of percent population of the sorted cells in the productive gate for each treatment at indicated concentrations (μM). Dilazep 30, 10μM and piceatannol 10μM show significant ($P<0.01$) increase in reactivation 0.5 μM SAHA, 0.5 μM prostratin and 0.5 ng/ml TNFα as compared to the reactivation obtained with these three drugs alone. TA also shows positive interaction with SAHA and prostratin at 10μM ($P<0.01$) and with SAHA at 3μM($P<0.05$). AG555 interact enhances reactivation mediated by prostratin and TNFα ($P<0.01$), whilst dipyridamole 30 and 10μM shows significant ($P<0.05$) positive interaction with prostratin only.

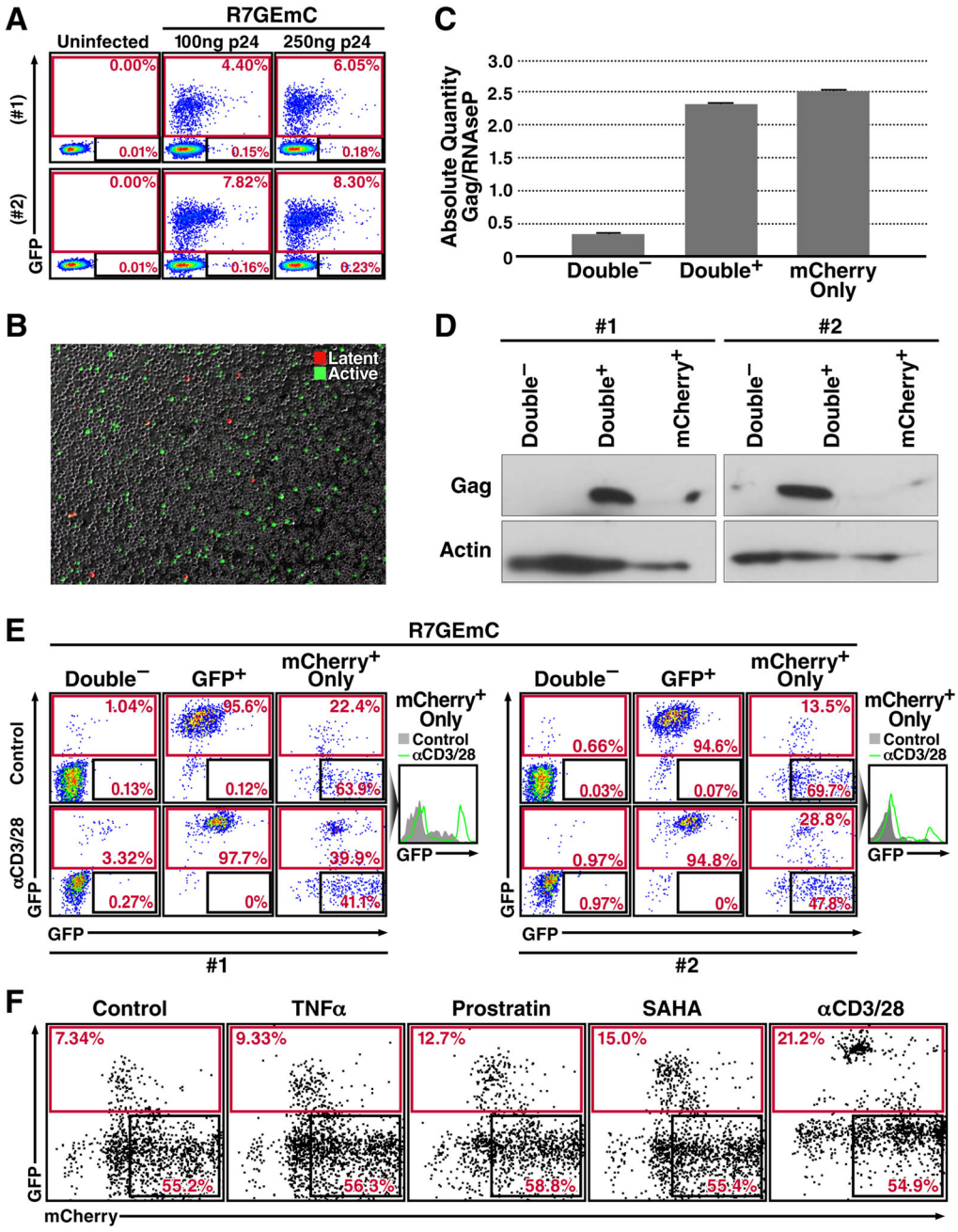

Figure 4. Two-Color Viruses Label a Population of Latently Infected Primary T Cells

(a) FACS analysis of activated CD4$^+$ T cells from two human donors (#1, #2) infected with R7GEmC at indicated virus amounts.

(b) Fluorescence microscopy image of infected CD4$^+$ T cells showing mCherry-positive (latent, red) and GFP-positive (active, green) cells.

(c) qPCR quantification of proviral DNA in the sorted populations, using primer-probe combinations for the HIV-1 *gag* gene and the *RNAseP* gene for normalization. Data represent mean ± SEM for three different donors.

(d) Western blot quantification of HIV *gag* and cell α-actin in sorted $CD4^+$ T cell populations from pooled donors.

(e) FACS analysis of sorted $CD4^+$ T cell populations from donors #1 and #2 after 48 h with anti-CD3/CD28-coated Dynabeads (αCD3/28) or left untreated (CTR). Right, histogram plot for the mCherry-only population of each donor in which the treated profile (green line) is overlaid on the untreated (grey shaded).

(f) Dot plot of mCherry-only population from three pooled donors treated with 10 ng/m, TNFα, 1 μM prostratin, 1 μM SAHA or anti-CD3/CD28-coated Dynabeads (1 bead/cell).